

Oscillating Pressure Experiments on Porcine Aorta

V. V. Romanov, S. Assari, and K. Darvish

Tissue Biomechanics Lab, College of Engineering, Temple University

ABSTRACT

This paper addresses the problem of Traumatic Aorta Rupture (TAR) that is one of the causes of fatality in motor vehicle accidents. The mechanisms that have been suggested for TAR are speculative and inconclusive and most tests performed have not been repeatable. One of the main reasons for these speculations is an incomplete understanding of the material properties of the aorta. The goal of the presented experiments is to characterize the relationship between stress and strain in the aorta wall in the biaxial pressure tests. An experimental setup was developed such that sinusoidal pressure (between 4.5 and 74.2 kPa) was supplied into porcine aorta at frequencies ranging from .5 Hz to 5 Hz. The aorta sample (n=7) was tested with both ends fixed and one end attached to the inlet tube for pressurization with normal saline solution. The deformation of aorta in the center and the pressure inside the aorta were recorded. The experimental results are represented in the form of Kirchhoff stress versus Green strain curves which show an increase in stiffness with an increase in the frequency. The curves also demonstrate that the loading and unloading paths of the aorta are different. The results of this study were then used to develop a material model of the aorta in biaxial loading conditions using the quasilinear viscoelastic theory.

INTRODUCTION

Traumatic Aorta Rupture (TAR), also known as Traumatic Rupture of Thoracic Aorta (TRA), is a major cause of deaths in motor vehicle collisions. According recent studies, TAR was diagnosed in 12% to 29% of autopsied fatally injured occupants. (Bertrand S, 2008) Furthermore, when people experience such trauma, only 9% (7500-8000 victims in US and Canada) survive from the scene of the accident and the overall mortality rate is 98%. (Richens D, 2002) In 94% of the cases, the shearing forces of high speed impacts have been associated with transverse tears at the peri-isthmic region which is subjected to the greatest strain. (Katyal, 1997)

Thoracic aorta consists of three major segments: ascending aorta, aortic arch, and descending aorta. Ascending aorta originates from the heart at the aortic valve. It then becomes the aortic arch which is suspended by the arteries that supply the blood to upper extremities. The descending aorta supplies the blood to the lower limb and is fixed to the spine with the intercostals arteries. The peri-isthmus region is located between the aortic arch and the descending aorta, at the point where the vessel becomes unattached from the spine. The general aortic anatomy is shown in Figure 1.

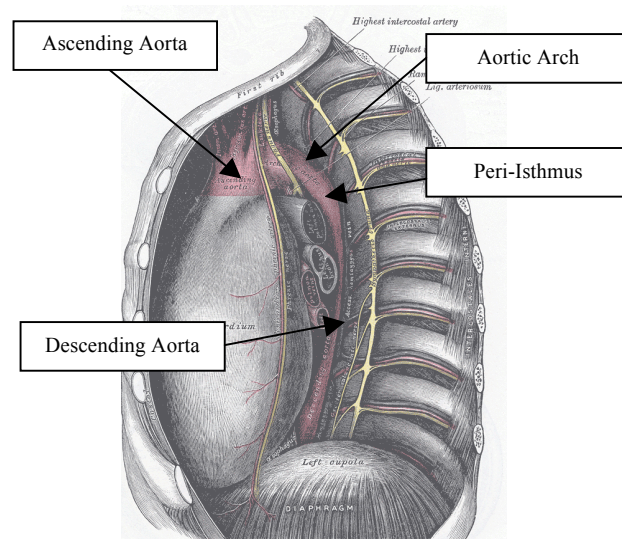


Figure 1: Anatomy of the Aorta (The Descending Aorta).

Several rupture mechanisms have been suggested in the literature. Presumably, the earliest proposal came from Rindfleisch, as cited by Richens, who suggested that the injury was caused by the sudden stretching of the aorta (Rindfleisch, 1893, Richens D, 2002). Therefore, as the body experiences a rapid deceleration, the heart moves forward creating stress between fixed descending aorta and aortic arch at the peri-isthmus. The second mechanism is the rupture due to pressure increase in the vessel when the thorax and the abdomen compress. Another mechanism proposed was the osseous pinch which suggests that the rupture of the aorta is caused by high local stress created by the pinch between highly compressed thorax and the spine (Richens D, 2002). However, though all of these mechanisms provide plausible explanations of rupture, a lot of the studies conducted are conflicting and insubstantial.

This study is one of the series with a common final goal to determine the most feasible cause of aortic rupture. The specific aim of this research is to understand the dynamic material

properties of the aorta through pressure oscillation tests. A noncontact experiment was developed to better understand the structural properties of the aorta in large deformations while keeping it intact.

METHODS

Experimental Procedure

For the experiments, seven samples from 6 month-old pigs were acquired from the local slaughter house. Porcine aorta was chosen because it has been widely used in the past in the cardiovascular related research as a substitute for a human aorta due to their similarities (Crick, 1998). Furthermore, human samples would have been difficult to obtain and it would have been highly unlikely that the samples would have been healthy.

To have all of the samples tested under the same conditions, aortas were ordered attached to the heart. Once received from the slaughter house, the samples were kept in saline solution at 5 °C until the beginning of the experiment. Throughout the test, the aorta was hydrated in the same solution but at the room temperature (25 °C).

Preparation work for each sample went through the same following procedure. The descending aorta was cut at 152mm from the aortic valve. The excessive fatty tissue was removed from the aorta. Once the tissue was removed, intercostal arteries were tied off at the base to prevent pressure loss.

To keep track of the geometrical changes, ultrasonic measurement sensors (Sonometrics Corp., Canada, 2R-34C-40-NB) were utilized. Each of the sensors sends and receives a pulse every 31ns to 2ms. Based on the speed of sound in the medium and the time of travel, Sonometrics software determined the distance between the two sensors with an accuracy of 30 μ m. Six sensors were sutured to the adventitia, the outside layer of the aorta.

The sensors were attached in pairs, on either side of the aorta. First pair of sensors was placed at 31mm from the cut edge. Second and third pair of sensors was then sutured at 22mm and 30mm, respectively, from the preceding pair. This position of the sensors allowed tracking the axial and transverse deformations of the vessel. Monitoring of these deformations allowed calculating the strains. Figure 2 below depicts the position sensors as they were placed on the aorta.

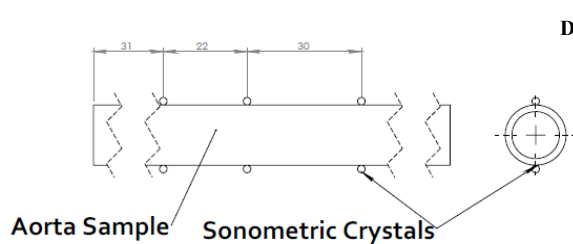


Figure 2: Sensor Position Diagram

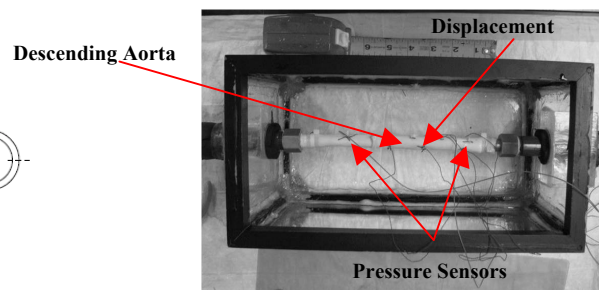


Figure 3: Sensor Position

To determine the pressure inside the vessel fiber optic pressure sensors (FISO Technologies Inc., Canada, FOP-MIV) were used. With a pressure accuracy of 0.1kPa, these sensors are designed based on the Fabry-Perot interferometer and use fiber optic cables to send the signal. One sensor was placed at each end of the vessel. Figure 3 above is the photograph of the sensor position.

Aorta was then attached to two tubes, one of which was sealed, while the other had a

connection available for the supply tank. Next, aorta was placed inside the test chamber and coupled to the supply tank. Saline was purged through the system, and also poured into the test chamber submerging the aorta. Figure 4 gives an example of the experimental setup.

The pressure was supplied through the air regulator from (Control Air Inc, USA, 550X). The regulator had a range of 0 psig to 30 psig (0kPa to 206.8kPa) which linearly corresponded to a current input 0mA to 20mA. Repeatability accuracy of the regulator was 2.07kPa. The pressure was applied in the form of a sinusoidal wave with a range of 7kPa to 76kPa and a frequency range of .5Hz to 5Hz. This specific pressure range was chosen to find the material properties that account for the maximum systolic and the failure pressures.

LabView program was used to control the current input and to record the output from the pressure sensors. Sonometrics software was used to record the deformation change of the vessel. To insure that the two programs recorded at the same time, a trigger was used to activate both of the programs. The entire experiment was also recorded using a high speed camera capable recording at 2200fps (Vision Research, USA).

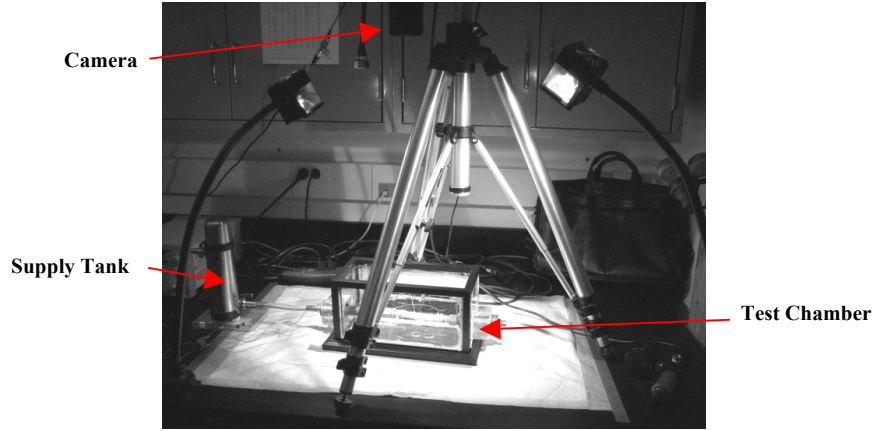


Figure 4: Experimental Setup

Hyperelasticity

Biological tissues have complex structures and are capable of undergoing large deformations. The stress-strain relationship of the tissue is in general nonlinear and the material exhibits hysteresis that would occur between the loading and unloading paths. The hysteresis is representative of the energy loss of the system. If the hysteresis can be assumed to be independent of the strain rate, then the material can be treated as nonlinear elastic, also known as pseudoelastic (Fung Y. C., 1975).

One of the more accepted ways to describe the stress-strain relationship of a pseudoelastic material is to utilize the exponential form of the hyperelastic strain energy function as the following (Fung Y. C., 1979).

$$\rho_o W = \frac{C}{2} \exp[a_1(E_{\theta\theta}^2 - E_{\theta\theta}^{*2}) + a_2(E_{zz}^2 - E_{zz}^{*2}) + 2a_4(E_{\theta\theta}E_{zz} - E_{\theta\theta}^*E_{zz}^*)] \quad (1)$$

The constants C (with units of stress) and a_1, a_2, a_3 (dimensionless) are the material constants. $E_{\theta\theta}^*, E_{zz}^*$ are the strains corresponding to a pair of stresses $S_{\theta\theta}^*, S_{zz}^*$ chosen to be the reference of the dynamic oscillations. The Green's strains are calculated by:

$$E_{\theta\theta} = \frac{1}{2}(\lambda_\theta^2 - 1); E_{zz} = \frac{1}{2}(\lambda_z^2 - 1) \quad (2)$$

where $\lambda_\theta, \lambda_z$ are the stretch ratios of the blood vessel in the circumferential and axial directions.

For this research, the radial stress can be considered negligible comparing to the stresses in the axial and circumferential directions (Fung Y. F., 1979, Bass, et al., 2001). Therefore, the arterial wall was considered as a two-dimensional body subjected only to Kirchhoff stresses $S_{\theta\theta}, S_{zz}$, which are defined as

$$S_{\theta\theta} = \frac{\sigma_{\theta\theta}}{\lambda_\theta^2} = \frac{\partial(\rho_o W)}{\partial E_{\theta\theta}}; S_{zz} = \frac{\sigma_{zz}}{\lambda_z^2} = \frac{\partial(\rho_o W)}{\partial E_{zz}} \quad (3)$$

Stresses $\sigma_{\theta\theta}, \sigma_{zz}$ can be found using the deformation data from the displacement sensors and utilizing Lamé's theory (Singh, 2008).

Quasi-linear Viscoelasticity

Quasi-linear viscoelasticity (QLV) was first proposed by Y.C. Fung, who noted that even though for small deformation linear viscoelasticity can be applied; for finite deformation the nonlinear stress-strain characteristic of the biological material must be considered. The QLV constitutive model for biaxial loading can be written as (Fung Y. , 1993):

$$S_{ij} = \int G_{ijkl} \frac{\delta S_{kl}^e[\mathbf{E}(\tau)]}{\delta \tau} \delta \tau \quad (4)$$

Where S_{ij} is the Kirchhoff's stress tensor, G_{ijkl} is the reduced relaxation tensor, and S_{kl}^e is the elastic stress corresponding to the strain tensor \mathbf{E} . Furthermore, S_{kl}^e can be approximated by a hyperelastic relationship discussed above.

For this study, it was assumed that the material was isotropic and that the axial and circumferential stresses had the same time dependency. The QLV model was implemented in the frequency domain and for biaxial loading equation 4 took the following form:

$$S_{\theta\theta} = G(f)[\alpha(S_{\theta\theta}^e + S_{zz}^e) + S_{\theta\theta}^e]; S_{zz} = G(f)[\alpha(S_{\theta\theta}^e + S_{zz}^e) + S_{zz}^e]; \quad (5)$$

α is a constant that couples the two stresses and has to be determined from the experimental data, while $G(f)$ is the reduced relaxation function written as:

$$G(f) = \sum_{j=1}^n \frac{G_j}{i2\pi f + \beta_i} + G_\infty \quad (6)$$

j corresponds to the number of terms that have to be present in the function, β_i is the constant that depends on the magnitudes of frequency, and G_i are the constants that have to be determined from the experimental data. In general, the number of terms in the equations depends on the orders of magnitude of frequency present in the experiment.

RESULTS

Pressure vs. Volumetric Strain Analysis

A hysteresis behavior was seen in the loading and unloading of the samples and the material also exhibited frequency dependency. These are the characteristics of the viscoelastic

material (Fung Y., 1993). To study the dependency of the material properties, Fast Fourier Transform (FFT) was used in LabView to extract the fundamental amplitude and phase for pressure and volumetric strain of the material. A linear modulus has been defined as the ratio of the pressure amplitude to the amplitude of volumetric strain at each frequency. The results showed an increase in linear modulus and phase shift as the frequency increased (Figures 5 and 6). This stiffening behavior confirmed the viscoelastic assumption.

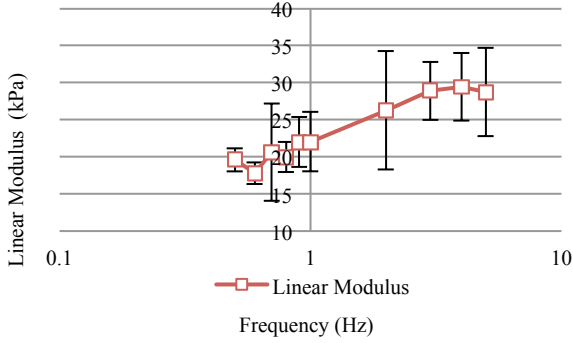


Figure 5: Frequency versus Linear Modulus

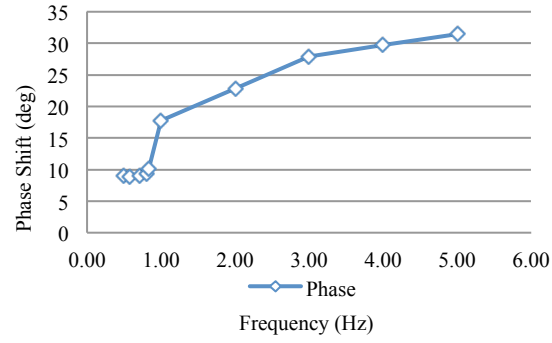


Figure 6: Frequency versus Phase Shift

Hyperelastic Modeling

The hyperelastic constitutive model was successful in modeling stress in both axial and circumferential directions at low frequencies, where the phase shift between the stress and the strain was small (Figure 7 and 8). The constants used for a sample hyperelastic model shown below are listed in Table 1.

Table 1 Constants of sample hyperelastic model

Frequency	C	a_1	a_2	a_4	$R^2(\theta)$	$R^2(z)$
.5	18.700	5.728	2.140×10^{-05}	4.864	0.994	0.994

As mentioned above, however, with higher strain rate phase shift increases, a condition that could not be predicted with the hyperelastic model alone. This is where the QLV modeling is utilized. Using the hyperelastic model for .5Hz as the nonlinear elastic function, a QLV constitutive equation was identified.

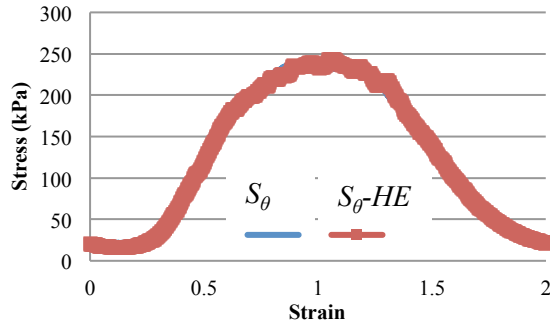


Figure 7: Circumferential Stress fit for 0.5 Hz

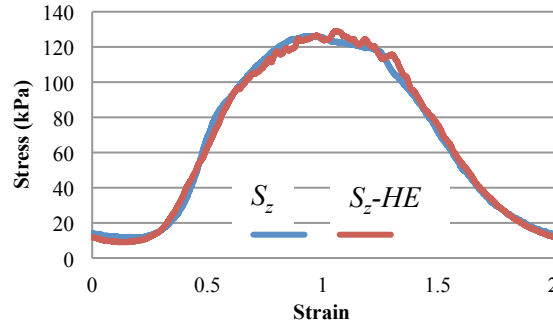


Figure 8: Axial Stress fit for 0.5 Hz

Viscoelastic Modeling

At this stage of the experiment only preliminary work has been performed and only one sample has been fitted. Its results are shown below in Figures 9, 10, and 11. The initial QLV model accounts well for the phase shift with an R^2 value of about .84 for both stresses. The amplitude matching, however, still needs further improvement. Even though the model fits the data well at 1Hz oscillation, at 0.5Hz the amplitude of the model stress and experimental stress do not match good while their trends are the same. Analysis of the rest of the samples (six) is underway to provide statistically significant results

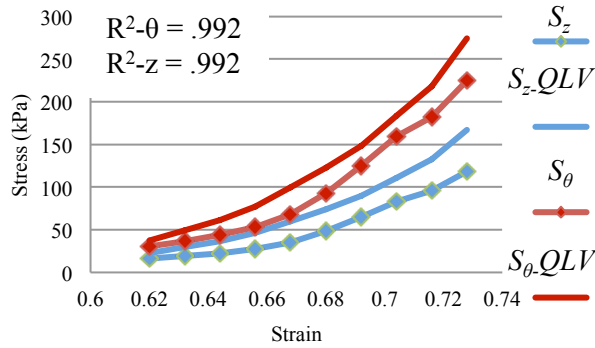


Figure 9: .5 Hz Input

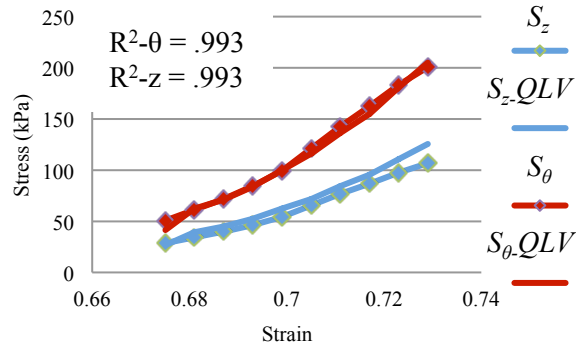


Figure 10: 1Hz Input

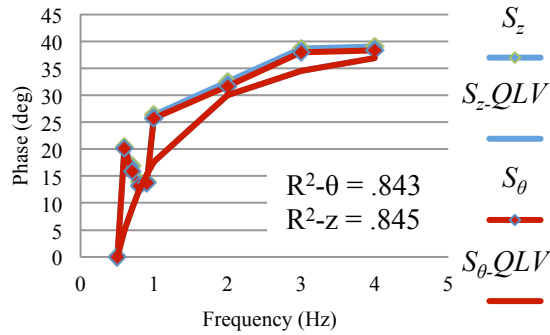


Figure 11: Phase Shift

CONCLUSIONS

This study was conducted to determine the dynamic properties of aorta under oscillatory pressure input. The Hyperelastic model provided a good fit at lower frequency, while at higher frequencies, a phase shift and change in amplitude between the model and the actual stresses were observed. To account for the two problems, the data was then modeled using a QLV constitutive equation. At this point only one sample has been fitted with the QLV constitutive equation. Although this preliminary study provided good matching between the experimental and model results, the rest of the samples (six) have to be fitted in order to provide statistically significant results.

ACKNOWLEDGEMENTS

The support for this study was provided by the NHLBI under Grant Numbers K25HL08651201 and R21 HL08815901 and Temple University College of Engineering.

REFERENCES

- Bass, C., Darvish, K., Bush, B., Crandall, J., Srinivasan, S., Tribble, C., et al. (2001). Material Properties for Modeling Traumatic Aortic Rupture. 45.
- Bertrand S, C. S. (2008). Traumatic Rupture of Thoracic Aorta in Real-World Motor Vehicle Crashes. *Traffic Injury Prevention*, 9 (2).
- Crick, S. J. (1998). Anatomy of the Pig Heart: Comparison with Normal Human Cardiac Structure. *Journal of Anatomy*, 193, 105-119.
- Fung, Y. (1993). *Biomechanics: Mechanical Properties of Living Tissues*. New York: Springer-Verlag New York, Inc.
- Fung, Y. C. (1975). On Mathematical Models of Stress-Strain Relationships for Living Soft Tissues. Riga: Plenum Publishing Corporation.
- Fung, Y. F. (1979). Pseudoelasticity of Arteries and the Choice of its Mathematical Expression. 237 (5).
- Katyal, D. M. (1997). Lateral Impact Motor Vehicle Collision: Significant Cause of Blunt Traumatic Rupture of the Thoracic Aorta. 42, 769-772.
- Richens D, F. M. (2002). The Mechanism of Injury in Blunt Traumatic Rupture of the Aorta. 42.
- Rindfleisch, E. (1893). Zur Entstehung und Heilung des Aneurysma Dissecans Aortae. 131, 374-.
- Singh, D. (2008). *Strength of Materials*. Boca Raton: CRC Press.
- The Descending Aorta*. (n.d.). (Yahoo! Education) Retrieved April 23, 2010, from <http://education.yahoo.com/reference/gray/subjects/subject/153>

AUTHOR LIST

1. Vasily V. Romanov
Address 1947 North 12th Street, Philadelphia, PA., 19122
Phone 215-204-9064
E-mail romanov@temple.edu
2. Soroush Assari
Address 1947 North 12th Street, Philadelphia, PA., 19122
Phone 215-204-9064
E-mail soroush.assari@gmail.com
3. Kurosh Darvish (Corresponding Author)
Address 1947 North 12th Street, Philadelphia, PA., 19122
Phone 215-204-3094
E-mail kdarvish@temple.edu